Power Sensitivity and Algebraic Technique for Evaluation of Penetration Level of Photovoltaic on DC Link of VSC HVDC Transmission

A F Nnachi[1], Prof J L Munda[1], IEEE Member,
[1]Department of Electrical Engineering
Tshwane University of Technology
Pretoria South Africa

Prof DV Nicolae[1], IEEE Member , Prof A Mpanda Mabwe[2], IEEE Senior Member
[2]Ecole superieure D'Ingenieurs en Electronique et Electrotechnique Amiens
France

***Abstract*—With the increased advent of VSC HVDC with long DC transmission link in power systems, situations have arisen and will be even more frequent in the future, where several distributed generation will be connected on the DC-link for more power transfer capability. As penetration level increases, there is need to predict the limit before violation of voltage and power instability on the DC transmission link and ensure that it does not interfere with the main VSC HVDC system control. In this paper, power sensitivity and algebraic technique is proposed to predict the maximum DG penetration that can be accepted at a particular location on the dc link of VSC HVDC transmission system before violation of voltage and power stability.**

Keywords- VSC-HVDC; Power sensitivity, algebraic technique, Multi-terminal, Distributed Generation

I. INTRODUCTION

From the advent of long overhead DC link of VSC HVDC transmission system, there has been much interest in connecting very large scale photovoltaic system or other distributed generation on the DC link resulting to multi-terminal system. Several literatures [1]-[4], have considered multi-terminal system on basis that the whole system is being planned and constructed at the same. Therefore they proposed different kinds of control strategy: those which use a master controller to specify certain control of some parameters and those which employ a coordinated control system where no master controller is required.

However, most of the VSC-HVDC systems are two-terminal and by tradition offers great advantage when used to strengthen a passive AC transmission network. They are designed such that the active and reactive power flow along HVDC lines can be controlled using the converter hardware at each end, potentially helping to avoid line congestion, and therefore saving investment in other parts of the network. This two terminal DC-link was generally not designed for connection of distributed generators.

When connecting a generating scheme to any transmission or distribution system, there certain technical issues that must be considered [5], [6]: thermal rating of equipment, system fault levels, stability, reverse power flow capability, line-drop compensation, steady-state voltage rise, losses, power quality (such as flicker, harmonics), protection. These issues are also applicable to connection of DGs on DC-link transmission system.

Before any distributed generator can be thought of being integrated on the VSC HVDC link transmission system, there is need to predict the maximum penetration level before violation of voltage and power instability on the DC transmission link. The type of instability problems will depend on the control parameter setting, converter ratings etc. In this paper, power sensitivity and a generalized algebraic method of determining maximum penetration level of PV on HVDC link is proposed.

II. FLEXIBLE CONFIGURATION OF MULT-TERMINAL VSC HVDC TRANSMISSION SYSTEMS

Future plans to introduce remote renewable power resources, such as very large scale PV or wind power on the DC link of Caprivi VSC HVDC transmission system have created interest in the possibility of an HVDC grid or multi-terminal HVDC. VSC multi-terminal HVDC system which consists of more than two voltage source converter stations connected together through a DC link can increase flexibility, DG penetration level, stability, transmission system capability and reliability. Power tap-offs along the length of the dc link to supply dispersed rural or electrification loads are also possible. Multi-terminal VSC HVDC systems can be radial, ring or meshed topologies [7] as shown in Fig. 1.

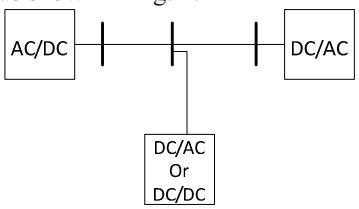

(a) Radial Multi-terminal HVDC

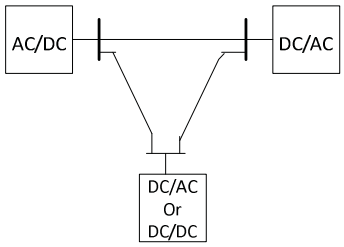

(b) Ring Multi-terminal HVDC

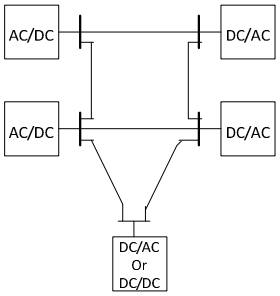

(c) Meshed Multi-terminal HVDC

Figure1. Flexible configuration of multi-terminal VSC HVDC systems

In this study, a radial DC multi-terminal system is envisaged. Before going further, a two terminal system is first investigated.

III. TWO-TERMINAL VSC HVDC TRANSMISSION SYSTEM

Fig. 2 shows a simplified model of Two-terminal VSC HVDC System.

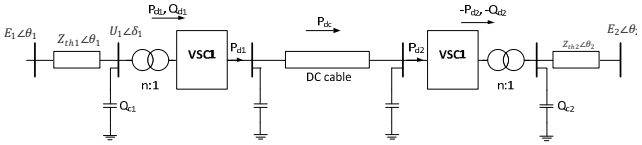

Figure 2. Simplified model of Two-terminal VSC HVDC System

A. Indices for the relative strengths of ac and dc systems

When planning to integrate distributed generation sources to the DC line of VSC HVDC link, certain factors need to be considered first. One of the most important factors is the strength of the AC network at the point at which the system couples. This strength will influence the design capacity of the scheme, controller design and performance of the scheme [8].

In order to get a measure of the strength of the AC system, the Short Circuit Ratio (SCR) is used as a guide. The AC system strength has a very significant impact in the ac/dc system interaction; it is therefore useful to have a simple means of measuring and comparing relative strength of ac systems. An index for the relative strengths of ac and dc systems is the short circuit ratio SCR defined as [9]:

Short-circuit ratio is defined as

$$SCR = \frac{Short-circuit\ level\ (MVA)\ of\ ac\ system}{Maximum\ power\ of\ dc\ link\ (MW)} \qquad (1)$$

The short circuit MVA is given by $SCR_{MVA} = \frac{E_{ac}^2}{Z_{th}}$ (2)

Where E_{ac} is the bus voltage at rated dc power and Z_{th} is the thevenin equivalent impedance of the ac system.
With all quantities expressed in p.u with the nominal DC-power and nominal AC voltage as base power and base voltage respectively,

$$SCR_{MVA} = \frac{1_{acp.u}^2}{Z_{th}} = \frac{1_{p.u}}{Z_{th(p.u)}} \qquad (3)$$

Therefore SCR is inversely proportional to the system impedance (at fundamental frequency). However once the converter stations are built, reactive support devices such as shunt capacitors and filters tend to decrease the fault level (or short circuit MVA) at the AC bus. Synchronous condensers however tend to increase the fault level at the ac bus. In order to cater for these devices the Effective Short Circuit Ratio (ESCR) is often calculated. Therefore, from the view point of the HVDC system performance, it is more meaningful to consider the effective short-circuit ratio (ESCR), which includes the effects of ac side equipment (filters, shunt capacitors, synchronous condensers, etc) associated with the dc link [9]. As shunt capacitors increase the system impedance seen by the converter, the effective short circuit ratio (ESCR) is defined as

$$ESCR = \frac{Short\ circuit\ level - Q_C}{Maximum\ dc\ link\ rating} = SCR - Q_{Cp.u} \qquad (4)$$

Where $Q_{Cp.u}$ in p.u of nominal dc power is the total MVA rating of AC filters and shunt capacitors connected at the ac bus [10], [11].

The value of ESCR greater than 5 indicates a strong ac system and a value between 3 and 5 is moderate and value less than 3 indicates a weak ac system. With refinement in dc and ac system controls, [12] recommends that ESCR greater than 3 indicates strong ac system, between 2 and 3 indicates weak system and less than 2 is very low.

B. Two-terminal dc circuit steady state modeling

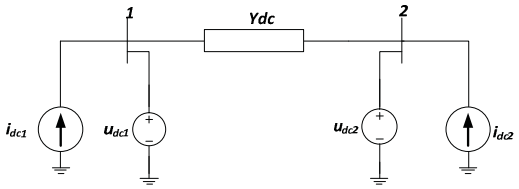

Figure 3. Equivalent circuit of 3-terminal VSC HVDC

Fig. 3 represents the DC-side of a two terminal VSC HVDC system, which consists of a large capacitor at converter

stations and a DC cable. The current injected at a DC bus 1 can be written as the current flowing to bus 2 as:

$$i_{dc1} = Y_{dc12}(u_{dc1} - u_{dc2}) \quad (5)$$

Therefore currents injected in the two dc bus network results to:

$$I_{dc} = Y_{dc}U_{dc} \quad (6)$$

Where $I_{dc} = [i_{dc1}\ i_{dc2}]^T$; $U_{dc} = [u_{dc1}\ u_{dc2}]^T$;

The DC-bus matrix

$$Y_{dc} = \begin{bmatrix} Y_{11} & -Y_{12} \\ -Y_{21} & Y_{22} \end{bmatrix} = \begin{bmatrix} Y_{dc} & -Y_{dc} \\ -Y_{dc} & Y_{dc} \end{bmatrix} \quad (7)$$

The active power injected in bus 1 and 2 from Jacobean matrix for monopolar DC grid can be written as

$$\left.\begin{aligned} P_{dc1} &= u_{dc1}i_{dc1} = u_{dc1}.Y_{dc}(u_{dc1} - u_{dc2}) \\ P_{dc2} &= u_{dc2}i_{dc2} = u_{dc2}.Y_{dc}(-u_{dc1} + u_{dc2}) \end{aligned}\right\} \quad (8)$$

Applying Newton Raphson method to power flow solutions, the nonlinear DC network equation from equation 8 can be solved with an NR method.

If the active power at each bus is specified, using superscript sp to denote specified values, we may write power flow equation:

$$\left.\begin{aligned} P_{dc1} &= P_{dc1}(u_{dc1}, u_{dc2}) = P_{dc1}^{sp} \\ P_{dc2} &= P_{dc2}(u_{dc1}, u_{dc2}) = P_{dc2}^{sp} \end{aligned}\right\} \quad (9)$$

The first step in the solution is to make initial estimates of all variables: u_{dc1}^{o}, u_{dc2}^{o}, where the superscript "o" indicates number of iteration cycles completed. Using these estimates, the power at each bus can be calculated from equation 8. These values are compared with the specified values to give a power error for bus 1 and 2 respectively as:

$$\left.\begin{aligned} \Delta P_{dc1}^{s} &= P_{dc1} - P_{dc1}(u_{dc1}^{o}, u_{dc2}^{o}) \\ \Delta P_{dc2}^{s} &= P_{dc2} - P_{dc2}(u_{dc1}^{o}, u_{dc2}^{o}) \end{aligned}\right\} \quad (10)$$

The power errors at each node are related to the errors in the dc voltage magnitudes Δu_{dc1}^{o}, Δu_{dc2}^{o}, by the first order approximation:

$$\Delta P_{dc} = J\Delta U_{dc} \quad (11)$$

Where $\Delta P_{dc} = \begin{bmatrix} \Delta P_{dc1}^{sp} \\ \Delta P_{dc2}^{sp} \end{bmatrix}, J = \begin{bmatrix} \frac{\partial P_{dc1}}{\partial u_{dc1}} & \frac{\partial P_{dc1}}{\partial u_{dc2}} \\ \frac{\partial P_{dc2}}{\partial u_{dc1}} & \frac{\partial P_{dc2}}{\partial u_{dc2}} \end{bmatrix}, U_{dc} = \begin{bmatrix} \Delta u_{dc1}^{o} \\ \Delta u_{dc2}^{o} \end{bmatrix}$

We can therefore easily compute the expected small changes in U_{dc} for changes in P_{dc} and the jacobian also provides every useful information regarding voltage sensitivity. The Jacobian matrix is a 2x2 because we have only two power controlled buses.

IV. 3-TERMINAL RADIAL VSC HVDC SYSTEM

The intention here is to connect a very large scale photovoltaic system on the dc link of the two-terminal HVDC link to form a radial 3-terminal system. Fig. 4 shows the equivalent circuit of 3-terminal VSC HVDC. Continuous injection of PV DC power on the dc line of the VSC HVDC link though will increase the power transfer capability of the system but should have a limit otherwise it lead to instability of the system.

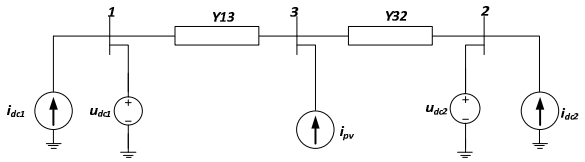

Figure 4. Equivalent circuit of 3-terminal VSC HVDC

A. Voltage and Power Stability

Voltage and power stability is a phenomenon that is of great concern in planning and operation of HVDC system especially when the HVDC converters are connected at ac system locations having low short circuit capacity. Voltage stability has been of concern in power industry during recent years and a number methods and tools have been developed. Voltage and power stability analysis in literatures [13]-[15] focused on single-feed and multi-infeed classical HVDC system. Two methods of analysis evolved are static approach which involves sensitivity techniques and dynamic approach (small signal & large signal technique).

B. Power sensitivity technique

In this study, power sensitivity technique is proposed for determination of penetration level limit of DG on DC-link of VSC HVDC transmission system. This is based on maximum avaliable power idea, which was first introduced by Ainsworth et al in [16] for a single-feed classical HVDC and extended to multi-infeed classical HVDC by [13]. In this case, this concept is adopted for VSC multi-terminal HVDC.

From figure 4, supposing that the maximum available dc power (MAP) VSC1 can deliver to the dc bus 3 which corresponds to i_{dc1MAP} is known. If Power is injected from the PV to bus 3, power delivered to VSC2 will increase. As currrent injection I_{PV} continue to increase, it will get to a point such that MAP of VSC1 will decrease and at such point, the system becomes unstable. Such a phenomenon corrsponds with unstable system behaviour, thus MAP of VSC1 condition determines the power stability and penetration limit of this radial multi-terminal VSC HVDC.

Mathematically this point corresponds to the condition that

$$\frac{dP_{dc1}}{dI_{PV}} = 0 \qquad (12)$$

Power flow studies are based on nodal voltage analysis of the power system. From the above figure, the nodal equation can be written directly.

In general for a system with r nodes, at node n, the current injected at node n i_n is written as

$$i_n = Y_{n1}V_1 + Y_{n2}V_2 + \cdots + Y_{nn}V_n + \cdots + Y_{nr}V_r = \sum_{k=1}^{r} Y_{nk}V_k$$

13

Where Y_{nn} = sum of all admittances connected to node n, Y_{nk} = -(sum of all admittances connected between nodes n & k) = Y_{kn}.

For the above three nodes,

$$\begin{bmatrix} i_{dc1} \\ i_{dc2} \\ i_{pv} \end{bmatrix} = \begin{bmatrix} y_{11} & y_{12} & y_{13} \\ y_{21} & y_{22} & y_{23} \\ y_{31} & y_{32} & y_{33} \end{bmatrix} \begin{bmatrix} u_{dc1} \\ u_{dc2} \\ u_{dc3} \end{bmatrix} \qquad (14)$$

Where y_{11}=Y_{13};$y_{12} = y_{21} = 0$; $y_{13} = y_{31} = -Y_{13}$; $y_{22} = Y_{32}$; $y_{23} = y_{32} = -Y_{32}$; $y_{33} = Y_{13} + Y_{32}$

From the Jacobian matrix, $i_{dc1} = u_{dc1}Y_{13} - u_{dc3}Y_{13}$

The active power injected at bus 1, 2 & 3 respectively for a monopolar DC grid can be written as:

$$\left.\begin{aligned} P_{dc1} &= u_{dc1}i_{dc1} \\ P_{dc2} = u_{dc2}i_{dc2} &= u_{dc2}(i_{dc1} + i_{pv}) \\ P_{dc3} &= u_{dc3}(i_{dc1} + i_{pv}) \end{aligned}\right\} \qquad (15)$$

The first step in the solution is to make initial estimates of all variables: $u_{dc1}^o, u_{dc2}^o, i_{dc1}^o, i_{pv}^o$, where the superscript "o" indicate number of iteration cycles completed. Using these estimates, the power at each bus can be calculated from equation 15. These values are compared with the specified values to give a power error for bus 1, 2 and 3 respectively as:

$$\left.\begin{aligned} \Delta P_{dc1}^o &= P_{dc1} - u_{dc1}^o i_{dc1}^o \\ \Delta P_{dc2}^o &= P_{dc2} - u_{dc1}^o(i_{dc1}^o + i_{pv}^o) \\ \Delta P_{dc3}^o &= P_{dc3} - u_{dc3}^o(i_{dc1}^o + i_{pv}^o) \end{aligned}\right\} \qquad (16)$$

The power errors at each node are related to the errors in the dc voltage and current magnitudes Δu_{dc1}^o, Δi_{dc1}^o, Δi_{pv}^o by the first order approximation:

$$\begin{bmatrix} \Delta P_{dc1}^o \\ \Delta P_{dc2}^o \\ \Delta P_{dc3}^o \end{bmatrix} = \begin{bmatrix} \frac{\partial P_{dc1}}{\partial u_{dc1}} & \frac{\partial P_{dc1}}{\partial i_{dc2}} & \frac{\partial P_{dc1}}{\partial i_{pv}} \\ \frac{\partial P_{dc2}}{\partial u_{dc1}} & \frac{\partial P_{dc2}}{\partial i_{dc1}} & \frac{\partial P_{dc2}}{\partial i_{pv}} \\ \frac{\partial P_{dc3}}{\partial u_{dc1}} & \frac{\partial P_{dc3}}{\partial i_{dc1}} & \frac{\partial P_{dc3}}{\partial i_{pv}} \end{bmatrix} \begin{bmatrix} \Delta u_{dc1}^o \\ \Delta i_{dc1}^o \\ \Delta i_{pv}^o \end{bmatrix} \qquad (17)$$

From 17 two approaches to analyze power stability of the system may be derived. The first approach is to focus on the

$$\frac{\Delta P_{dc1}^o}{\Delta i_{pv}^o} = \Delta u_{dc1}^o \frac{\partial P_{dc1}}{\partial u_{dc1}} + \Delta i_{dc1}^o \frac{\partial P_{dc1}}{\partial i_{dc2}} + \Delta i_{pv}^o \frac{\partial P_{dc1}}{\partial i_{pv}} \qquad (18)$$

When $\Delta i_{pv}^o \frac{\partial P_{dc1}}{\partial i_{pv}}$ becomes zero, it will be seen that the radial multi-terminal VSC HVDC system reaches a condition akin to the MAP of VSC1 condition defined in 12. This yields power stability boundary of this system and hence maximum penetration level of the PV system. From power flow solution, i_{pvmax} will be determined.

V. ANALYTICAL METHOD FOR EVALUATION OF MAXIMUM PENETRATION LEVEL

In this section, the proposed algebraic method is presented. This method is simple and better since it only needs the control and dc link parameter to predict or estimate the penetration limit.

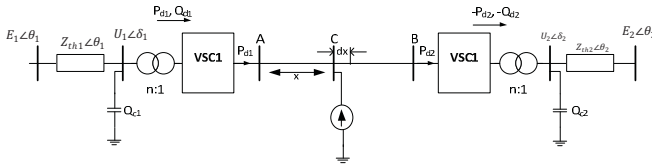

Figure 5 Simplified model of radial Three-terminal VSC HVDC System

Fig. 5 shows a VSC HVDC with a long DC link AB of length L, VSC1 as rectifier and VSC2 as inverter, with DG power injection at bus 3.
VSC1 and VSC2 controller designs are identical. The two controllers are independent with no communication between them. Each converter has two degrees of freedom.

Without introduction of the PV, Pdc1 flows into bus 2 and give rise to a voltage drop between bus 1 and bus 2. The introduction of a DG on bus 3 and increasing its power injection could reach an extent (high DG output) that the direction of flow of power Pdc1 could be reversed and these will cause a net voltage rise of bus bar 3 with respect to bus 1.
Using the principle of uniform loading [17], the maximum penetration level of distributed generation (DG in this case is PV system) can be analytically derived as follows:

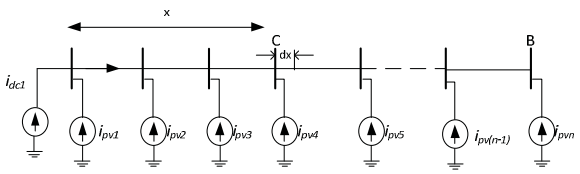

Figure 6. Uniformly distributed generation on DC-link of VSC HVDC transmission system

From Fig. 6, Let i_{pv} be current injected per unit length, i_{dc1} – the dc current from the inverter to bus 1, L – the total length of the HVDC link, r – resistance per unit length of the link. At any point,

$$i = i_{dc1} + \sum_{j=1}^{n} i_{pvj} \tag{19}$$

Now, let us find the voltage rise at point C which is at a distance x units from A.
Consider a small section of length *dx* near point *c*, its resistance is *rdx*; hence voltage rise over length dx is

$$dv = i(L-x)rdx = (iLr - ixr)dx \tag{20}$$

The total rise up to the point x is given by integrating the above quantity between proper limits

$$\int_0^V dv = \int_0^x (iLr - ixr)dx \tag{21}$$

$$V_{x\_rise} = iLrx - \frac{1}{2}irx^2 = ir\left(Lx - \frac{x^2}{2}\right) \tag{22}$$

The drop or rise at point B can be obtained by putting x = L in the expression so that

$$V_{B\_rise} = ir\left(L^2 - \frac{L^2}{2}\right) = \frac{irL^2}{2} = \frac{iL \times rL}{2} = \frac{1}{2}IR_{Line} \tag{23}$$

Equation 22 shows that the voltage rise of a uniformly injected distributed generation at a point *x* on the dc-link is a parabola. Equation 23 shows that the total voltage rise is equal to that produced by the whole of the DG assumed connected at the middle point. Therefore, it is significant that in the worst case – the whole DG is installed at end of the link (B) and this case the length will be assumed to be doubled. Therefore, at this point B i.e. length 2L, if the total power or maximum power transferred to the ac side of the inverter load is Pdc2, then at point x i.e 2L-x from B the power transferred will be

$$\frac{2L-x}{2L}P_{dc2} = \left(1 - \frac{x}{2L}\right)P_{dc2}.$$

At point x,

$$\frac{V_1 - V_3}{rx} + i_{pv} = \frac{V_3 - V_2}{r(L-x)} \tag{24}$$

$$V_3 i_{pv} = P_{pv} = \frac{-V_3(V_3 - V_1)}{rx} + \frac{V_3(V_3 - V_2)}{r(L-x)} \tag{25}$$

$$P_{pv} = \frac{-V_3(V_3 - V_1)}{rx} + \left(1 - \frac{x}{2L}\right)P_{dc2} \tag{26}$$

But neglecting inverter losses,

$$P_{dc2} = U_{dc2}I_{dc2} = P_{ac2} = \frac{U_2 E_2}{X_{th}} sin\delta \tag{27}$$

$$P_{pv} = -\frac{V_3(V_3 - V_1)}{rx} + \left(1 - \frac{x}{2L}\right)U_{dc2}I_{dc2} \tag{28}$$

With V_3 being the upper voltage regulation limit on the dc link and V_1 being the setpoint or reference voltage and all values in per unit,

$$P_{pv} = -\frac{U_{dcmax}(U_{dcmax} - U_{dcref})}{rx} + \left(1 - \frac{x}{2L}\right)U_{dc2}I_{dc2} \tag{29}$$

Where
U_{dcmax} = the upper voltage regulation limit in p.u specified in the control
U_{dcref} = the reference voltage in p.u
r = resistance per unit length of the line
x = distance of from bus 1
L = Total length of the DC-link
U_2 = converter AC output voltage
E_2 = AC bus voltage
X_{th} = the thevenin equivalent reactance of the ac system
U_{dc2} = p.u the upper voltage regulation (limit in p.u specified in the inverter control)
$I_{dc2} = I_{rated}$ = p.u current reference limit (current set point specified in the inveter control)

VI. Simulation Validation

In this paper, the emphasis is not placed on the control scheme rather a standard control [18] of VSC HVDC and its control settings are utilized. From control setting parameters of existing two-terminal VSC HVDC transmission system in Simulink with Dc-link of 150 km the following parameters were used: $U_{dcmax} = 1.05\,p.u$; $U_{dcref} = 0.95$; $U_{dc2} = 1.05\,pu$; $I_{dc2} = 1$; $r = 0.0139\,pu\ of\ km$.

The simulation were carried by injecting PV on the midpoint of the dc-link (x=75 km). From Fig. 7, it will be seen that as power injection increases, power transfer from VSC1 remains constant (0.86 pu) until a point of penetration limit of 0.6 pu, then it start to drop. Also Fig. 8 shows the voltages of bus 1 and bus 2 which remained constant as penetration increases until at a point they starts to increase. Therefore, penetration limit when PV is connected at the middle point of the DC-link is seen by simulation to be 0.6.
From our algebraic equation 29, substituting the control and dc-link parameters, the penetration limit is calculated thus:

$$P_{pvmax} = -\frac{1.05(1.05 - 0.95)}{1.39 \times 10^{-2} \times 75} + \left(1 - \frac{75}{2x150}\right) \times 1.05 \times 1$$

= 0.68 p.u
The PV penetration level is therefore defined as:

$$\%PV_{penetration-level} = \frac{P_{pv}}{P_{dc1}+P_{pv}} \times 100 \quad (29)$$

Where P_{dc1} is the maximum dc power VSC1 can deliver to the dc bus 3 is known (Known as maximum avaliable power MAP) and P_{pv} is the total power generated by the PV and injected at bus 3.

Therefore from simulation,

$$\%PV_{penetration-level} = \frac{0.6}{0.86 + 0.6} \times 100 = 41\%$$

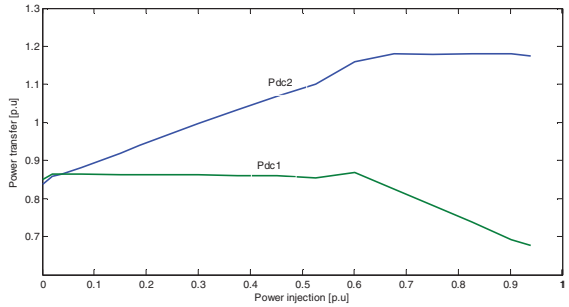

Figure 7. Effect of increasing penetration level on power transfer of VSC1 and VSC2

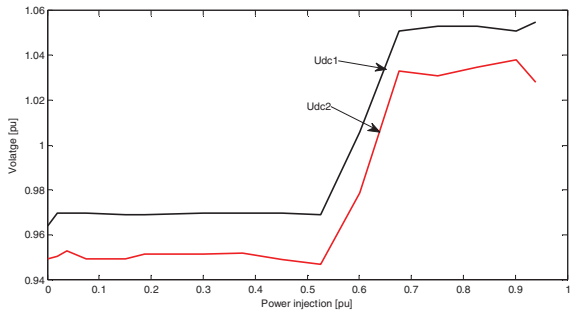

Figure 8. Effect of increasing penetration level on DC-bus voltage of VSC1 and VSC2

VII. CONCLUSION

The recent development in VSC HVDC transmission system will pave way for integration of renewable sources (multi-wind-farm and PV systems) to the DC-link through multi-terminal system. As penetration level increases, there is need to predict the limit before violation of voltage and power instability on the DC transmission link and ensure that it does not interfere with the main VSC HVDC system control. In this paper, power sensitivity based on maximum available power theory and algebraic technique based on uniformly distributed generation scheme is proposed to predict penetration limit. Simulation results validate the algebraic technique of penetration limit prediction.

REFERENCES

[1] DU, C., Bollen, M. H., Agneholm, E., & Sannino, A. (2007). A new control strategy of a VSC-hvdc system for high quality supply of indutrial plant. IEEE Transactions on Power Delivery, 22, pp. 2386-2394.

[2] Xingjia Yao, Hongxia Sui, Zuoxia Xing, "The Study of VSC-HVDC Transmission System for Offshore Wind Power Farm," in Proc.2007 international conference on electrical machines and systems, pp.314-319

[3] Li Gengyin, Yin Ming, Zhou Ming Zhao Chengyong. "Decoupling Control for Multi-terminal VSC-HVDC Based Wind Farm Interconnection, " in Proc. 2007 Power Engineering Society General Meeting, pp.1-6

[4] Ruihua Song, Chao Zheng. "Vscs based HVDC and its Control Strategy". in Proc.2005 IEEE/PES Transmission and Distribution Conference & Exhibition, pp.1-6

[5] Masters, C. L. (2002, Feb). Voltage rise: the big issue when connecting embedded generation to long 11 kV overhead lines. IEE Power Engineering Journal, 16, 5-12.

[6] Van Zyl, S., & Gaunt, C. (2005). A generalised method for evaluating voltagr rise in DG-equiped networks . Cigre SC-C6 Colloquium. Cape Town.

[7] Johansson, S. G., Asplund, G., Jansson, E., & Rudervall, R. (2004). Power System Stability Benefits with VSC DC-Transmision System. CIGRE Conference. Paris France.

[8] Coker, M., & Chown, G. M. (2006). Eskom Research Report.

[9] Kundur, P. (1993). Power System Stability and Control. United states: McGraw-Hill.

[10] Denis, L. H., & Goran, A. (1997). Voltage stability analysis of multi-infeed HVDC System. IEEE Transaction on Power Delivery, 12, pp. 1309-1318.

[11] Jape, V., Lokhande, N., & Khatri, P. (2006). Simulation of HVDC system connected to AC Buses in Close Proximity. IEEE, (pp. 2137 - 2141).

[12] CIGRE and IEEE Joint Task Force Report. (1992). Guide for planning DC Links Terminating at AC Locations Having Low Short-Circuit Capacities, Part 1: AC/DC Interaction Phenomena. CIGRE Publication 68.

[13] Denis, L. H. (2000). Methods for Voltage and Power Stability Analysis of Emerging HVDC System Configurations . IEEE, (pp. 409-414).

[14] Hammad, A. E., Sadek, K., & Kauferle, J. (1984). A new Aproach for the Analysis of and solution of AC voltage stability Problems at HVDC terminal. Proceedings on international Conference on DC Power Transmission, (pp. 164 - 170). Montreal, Canada.

[15] Lee, H. A., & Denis, A. (1999). Nonlinear Dynamics in HVDC Systems. IEEE Transactions on Power Delivery, 14, pp. 1417 - 1426.

[16] Ainsworth, J. D., Gavrilovic, A., & Thanawala, H. L. (1980). Static and Synchronous Compensations for HVDC Transmission Converters Connected to weak AC Systems. Cigre General Session. Paris, France.

[17] Arijit, B., Arindam, m., Mark, H., & Joe, S. E. (2003). Determination of allowable penetration levels of distributed generation resources based on harmonic limit considerations. IEEE Transactions on power delivery, 18, pp. 619 - 624.

[18] Jiuping P., Renaldo N., Le T., and Per H. (2008). VSC-HVDC Control and application in meshed AC network. . IEEE-PES General meeting. Pittsburgh Pennsylvania.